Generator-coordinate reference states for spectra and $0\nu\beta\beta$ decay in the in-medium similarity renormalization group

J. M. Yao

Department of Physics and Astronomy, University of North Carolina, Chapel Hill, North Carolina 27516-3255, USA
and FRIB/NSCL, Michigan State University, East Lansing, Michigan 48824, USA

J. Engel and L. J. Wang

Department of Physics and Astronomy, University of North Carolina, Chapel Hill, North Carolina 27516-3255, USA

C. F. Jiao

Department of Physics and Astronomy, University of North Carolina, Chapel Hill, North Carolina 27516-3255, USA
and Department of Physics, San Diego State University, San Diego, California 92182-1233, USA

H. Hergert

FRIB/NSCL and Department of Physics and Astronomy, Michigan State University, East Lansing, Michigan 48824, USA

We use a reference state based on symmetry-restored states from deformed mean-field or generator-coordinate-method (GCM) calculations in conjunction with the in-medium similarity-renormalization group (IMSRG) to compute spectra and matrix elements for neutrinoless double-beta ($0\nu\beta\beta$) decay. Because the decay involves ground states from two nuclei, we use evolved operators from the IMSRG in one nucleus in a subsequent GCM calculation in the other. We benchmark the resulting IMSRG+GCM method against complete shell-model diagonalization for both the energies of low-lying states in ^{48}Ca and ^{48}Ti and the $0\nu\beta\beta$ matrix element for the decay of ^{48}Ca, all in a single valence shell. Our approach produces better spectra than either the IMSRG with a spherical-mean-field reference or GCM calculations with unevolved operators. For the $0\nu\beta\beta$ matrix element the improvement is slight.

I. INTRODUCTION

The search for neutrinoless double-beta ($0\nu\beta\beta$) decay is an important effort in modern nuclear and particle physics, in part because it offers the only real hope of determining whether neutrinos are Majorana particles [1,2]. The rate of decay, however, depends on nuclear matrix elements that must be accurately calculated to allow experimentalists to plan efficiently and interpret results. At present, the matrix elements predicted by various nuclear models [3–15] differ by factors of up to 3 [16]. Theorists have worked hard to identify the shortcomings of the models and improve them accordingly. Ultimately, however, we will need fully *ab initio* calculations with controlled uncertainty.

Ab initio methods have improved rapidly in recent years [17–24]. Most applications, however, are still in relatively light nuclei near closed shells. The nuclei used in $\beta\beta$ experiments, among them ^{76}Ge, ^{82}Se, ^{130}Te, ^{100}Mo, ^{136}Xe, and ^{150}Nd, are typically heavier and often far from closed shells in protons, neutrons, or both. Among the existing *ab initio* methods, the in-medium similarity renormalization group (IMSRG) method [24–26] is particularly suited to an extension to such mid-shell nuclei. One scheme for making the extension involves choosing the generators of the RG flow to decouple a shell-model space from the rest of the full

many-body Hilbert space [27–30]. Although the framework, called the valence-space IMSRG, has been used to describe nuclei as heavy as tin [31], it suffers from the use of a closed-shell reference state or a spherical reference ensemble, both of which omit collective correlations [32]. Such correlations are difficult to capture in an approximate SRG flow that simplifies induced many-body operators.

In the IMSRG as currently practiced, induced A-body operators with $A > 2$ are included only approximately by retaining just their normal-ordered one- and two-body pieces. Collective effects will be better represented if they are explicitly built into the reference state. To use a more general reference state, one must extend the procedure of normal ordering. References [33–35] show how to define a normal ordering that applies to any reference state; the work of Refs. [36,37] made use of the scheme with a number-projected spherical Hatree-Fock-Bogoliubov reference state (which explicitly includes pairing correlations) to apply the IMSRG to spherical open-shell isotopes. More recently, the authors of Ref. [38] used a no-core shell-model reference state in just a few shells (for lighter nuclei). They showed that the IMSRG flow with respect to that reference generates a Hamiltonian for subsequent calculations in the same few shells that effectively incorporates the physics from many higher shells.

In this paper, we generalize the reference state even further, not only by including angular-momentum-projected Hartree-Fock-Bogoliubov (HFB) states with deformation, but also by using the generator-coordinate method (GCM) to mix many such states, so that the IMSRG can be applied to essentially any nucleus. The GCM is flexible enough to include in the reference both the "static" correlations associated with collectivity—superfluidity and deformation—and "dynamic" correlations associated with shape fluctuations. The IMSRG flow then incorporates noncollective correlations, generating an improved Hamiltonian that we use in a second GCM calculation and evolved transition operators with which to obtain other nuclear properties. Here we focus not only on energy spectra, but also on the $0\nu\beta\beta$ transition matrix elements, and show how to include the effects of complicated noncollective correlations in that process. We then benchmark the method against the conventional shell model for the spectra of ^{48}Ca and ^{48}Ti and the transition matrix element between the two.

The paper is organized as follows. In Sec. II we present the IMSRG+GCM method for computing both the energies of low-lying states and the matrix elements for $0\nu\beta\beta$ decay, and use ^{48}Ca and ^{48}Ti within a valence shell to illustrate the method. Section III presents and discusses the results. Section IV offers a summary and some perspective.

II. FORMALISM

In this section we present a general framework for the IMSRG+GCM. Although we restrict our calculations to a single shell with a phenomenological Hamiltonian here, all the expressions we develop are more general. We will report their application within an *ab initio* calculation, with interactions from chiral effective field theory, in a separate paper.

A. The IMSRG

The basic idea of the IMSRG is to use a flow equation to gradually decouple a chosen reference state $|\Phi\rangle$ (or more generally a space or ensemble) from all other states. One defines a Hamiltonian $H(s)$ that depends on a flow parameter s as

$$\hat{H}(s) = \hat{U}(s)\hat{H}_0\hat{U}^\dagger(s), \tag{1}$$

with $\hat{U}(0) = 1$, where $\hat{H}_0$ is the initial Hamiltonian and $\hat{U}(s)$ represents a set of continuous unitary transformations that drive $\hat{H}_0$ to a specific form, e.g., by eliminating certain matrix elements or minimizing its expectation value. Taking the derivative d/ds of both sides of Eq. (1) yields the flow equation

$$\frac{d\hat{H}(s)}{ds} = [\hat{\eta}(s), \hat{H}(s)], \tag{2}$$

where we have introduced the anti-Hermitian generator of the transformation,

$$\hat{\eta}(s) \equiv \frac{d\hat{U}(s)}{ds}\hat{U}^\dagger(s). \tag{3}$$

Supposing the Hamiltonian $\hat{H}$—either $\hat{H}_0$ or an approximate $\hat{H}(s)$—is composed of one-body, two-body and three-body terms, and writing strings of creation and annihilation operators as

$$A^{pqr\cdots}_{stu\cdots} = a^\dagger_p a^\dagger_q a^\dagger_r \ldots a_u a_t a_s, \tag{4}$$

we have

$$\hat{H} = \sum_{pq} t^p_q A^p_q + \frac{1}{4}\sum_{pqrs} V^{pq}_{rs} A^{pq}_{rs} + \frac{1}{36}\sum_{pqrstu} W^{pqr}_{stu} A^{pqr}_{stu}. \tag{5}$$

Using the generalized normal ordering of Kutzelnigg and Mukherjee [33–35], we can normal-order $\hat{H}$ with respect to our arbitrarily chosen reference state $|\Phi\rangle$:

$$\hat{H} = E + \sum_{pq} f^p_q \{A^p_q\} + \frac{1}{4}\sum_{pqrs} \Gamma^{pq}_{rs} \{A^{pq}_{rs}\}$$
$$+ \frac{1}{36}\sum_{pqrstu} W^{pqr}_{stu} \{A^{pqr}_{stu}\}. \tag{6}$$

By definition, the expectation values of normal-ordered operators, indicated by $\{A^{p\cdots}_{q\cdots}\}$, with respect to the reference state are zero. Thus, the normal-ordered zero-body term corresponds to the reference-state energy E, which is given by

$$E = \langle\Phi|\hat{H}|\Phi\rangle = \sum_{pq} t^p_q \rho^p_q + \frac{1}{4}\sum_{pqrs} V^{pq}_{rs} \rho^{pq}_{rs}$$
$$+ \frac{1}{36}\sum_{pqrstu} W^{pqr}_{stu} \rho^{pqr}_{stu}. \tag{7}$$

The normal-ordered one-body and two-body terms are

$$f^p_q = t^p_q + \sum_{rs} V^{pr}_{qs} \rho^r_s + \frac{1}{4}\sum_{rstu} W^{prs}_{qtu} \rho^{rs}_{tu}, \tag{8}$$

$$\Gamma^{pq}_{rs} = V^{pq}_{rs} + \sum_{tu} W^{pqt}_{rstu} \rho^t_u. \tag{9}$$

In Eqs. (7)–(9), we have introduced the usual density matrices

$$\rho^p_q = \langle\Phi|A^p_q|\Phi\rangle, \tag{10a}$$
$$\rho^{pq}_{rs} = \langle\Phi|A^{pq}_{rs}|\Phi\rangle, \tag{10b}$$
$$\rho^{pqr}_{stu} = \langle\Phi|A^{pqr}_{stu}|\Phi\rangle. \tag{10c}$$

Correlations within the reference state are encoded in the corresponding *irreducible* density matrices (also referred to as cumulants):

$$\lambda^p_q = \rho^p_q, \tag{11a}$$
$$\lambda^{pq}_{rs} = \rho^{pq}_{rs} - \mathcal{A}(\lambda^p_r \lambda^q_s) = \rho^{pq}_{rs} - \lambda^p_r \lambda^q_s + \lambda^p_s \lambda^q_r, \tag{11b}$$
$$\lambda^{pqr}_{stu} = \rho^{pqr}_{stu} - \mathcal{A}(\lambda^p_s \lambda^{qr}_{tu} + \lambda^p_s \lambda^q_t \lambda^r_u), \tag{11c}$$

where the antisymmetrization operator $\mathcal{A}$ generates all possible permutations (each only once) of upper indices and lower indices. For independent particle states, the two-body irreducible density vanishes and we recover the usual factorization of many-body density matrices into antisymmetrized products of the one-body density matrix.

To decouple $|\Phi\rangle$, one usually chooses an appropriate generator $\hat{\eta}$ and then solves a set of coupled ordinary differential equations (ODEs), derived from Eq. (2), for $\hat{f}$, $\hat{\Gamma}$, … [26,36]. Instead, however, one can solve a similar flow equation for the unitary transformation operator $\hat{U}(s)$,

$$\frac{d\hat{U}(s)}{ds} = \hat{\eta}(s)\hat{U}(s), \tag{12}$$

whose solution can formally be written in terms of the $\mathcal{S}$-ordered exponential

$$\hat{U}(s) = \mathcal{S}\exp\int_0^s ds'\hat{\eta}(s'), \tag{13}$$

which is shorthand for the Dyson series expansion of $\hat{U}(s)$. As shown first by Magnus [39,40], if certain convergence conditions are satisfied it is possible to write $\hat{U}(s)$ as a proper exponential of an anti-Hermitian operator $\hat{\Omega}(s)$:

$$\hat{U}(s) \equiv e^{\hat{\Omega}(s)}. \tag{14}$$

Equation (12) can then be reexpressed as a flow equation for $\hat{\Omega}$:

$$\frac{d\hat{\Omega}(s)}{ds} = \sum_{n=0}^{\infty}\frac{B_n}{n!}[\hat{\Omega}(s), \hat{\eta}(s)]^{(n)}, \tag{15}$$

where we define nested commutators as

$$[\hat{\Omega}(s), \hat{\eta}(s)]^{(0)} = \hat{\eta}(s), \tag{16a}$$

$$[\hat{\Omega}(s), \hat{\eta}(s)]^{(n)} = [\hat{\Omega}(s), [\hat{\Omega}(s), \hat{\eta}(s)]^{(n-1)}], \tag{16b}$$

and $B_{n=0,1,2,3,\dots}$ are the Bernoulli numbers $\{1, -1/2, 1/6, 0, \dots\}$. As discussed in Ref. [41], the reformulation of the IMSRG via the Magnus expansion has two major advantages. First, the anti-Hermiticity of $\hat{\Omega}$ guarantees that $\hat{U}(s)$ is unitary throughout the flow, even when low-order numerical ODE solvers are used to integrate Eq. (15). Second, it greatly facilitates the evaluation of observables. In the traditional approach, we would need to solve flow equations for each additional operator *simultaneously* with Eq. (2) because of the dynamical nature of the generator, while $\hat{\Omega}(s)$ allows us to construct arbitrary evolved operators by using the Baker-Campbell-Hausdorff (BCH) formula:

$$\hat{O}(s) = e^{\hat{\Omega}(s)}\hat{O}(0)e^{-\hat{\Omega}(s)} = \sum_{n=0}^{\infty}\frac{1}{n!}[\hat{\Omega}(s), \hat{O}(0)]^{(n)}. \tag{17}$$

As mentioned earlier, the IMSRG generator $\hat{\eta}(s)$ is chosen to implement a specific decoupling. For closed-shell nuclei, the ability to use an uncorrelated reference allows us to distinguish particle and hole states, which simplifies the formulation of decoupling conditions [24,25], and the subsequent construction of $\hat{\eta}(s)$. For correlated reference states like those we aim to use here, this distinction is lost, and one needs to carefully consider the proper generalization of the generator. Here, we use the Brillouin generator, which is essentially the gradient of the energy under a general unitary transformation

(see Appendix B and Ref. [25]):

$$\eta_q^p \equiv \langle\Phi|[\hat{H}, \{A_q^p\}]|\Phi\rangle, \tag{18a}$$

$$\eta_{rs}^{pq} \equiv \langle\Phi|[\hat{H}, \{A_{rs}^{pq}\}]|\Phi\rangle. \tag{18b}$$

To implement the IMSRG flow either in the traditional [Eq. (2)] or Magnus formulations [Eq. (15)], we need to close the system of flow equations by truncating the operators at a given particle rank. We adopt the IMSRG(2) approximation and truncate $\hat{H}(s)$, $\hat{\eta}(s)$, and $\hat{\Omega}(s)$, as well as all commutators, at the normal-ordered two-body level. This is consistent with the so-called NO2B approximation that is applied to the input Hamiltonian in a variety of many-body approaches (see, e.g., [42–45]). With this choice of operator truncation, up to three-body irreducible density matrices of the reference states appear in the Brillouin generator and the flow equations. We will show that the irreducible three-body density in the Brillouin generator is vital to the convergence of the IMSRG(2) flow equations.

B. Choice of reference state

We would like to explore reference states $|\Phi\rangle$ that incorporate collective (or "static") correlations, such as those associated with pairing and deformation, plus fluctuations in some of these collective quantities. To include such correlations, we use the GCM to find an optimal linear combination of deformed HFB states (distinguished from one another by a set of coordinates $\mathbf{q}$), projected onto states with both well-defined neutron (N) and proton (Z) number and angular momentum $J = 0$:

$$\left|\Phi_\alpha^{J=0}\right\rangle = \sum_{\mathbf{q}} f_\alpha^{J=0}(\mathbf{q})|NZJ=0, \mathbf{q}\rangle, \tag{19}$$

where α denotes a particular linear combination, and the nonorthogonal basis states in which the GCM states are expanded are given by

$$|NZJ=0(\mathbf{q})\rangle = \hat{P}^N\hat{P}^Z\hat{P}_{00}^{J=0}|\mathbf{q}\rangle. \tag{20}$$

Here, the particle-number projection operator is

$$\hat{P}^\tau = \frac{1}{2\pi}\int_0^{2\pi} d\varphi_\tau e^{i(\hat{N}_\tau - N_\tau)\varphi_\tau}, \tag{21}$$

with $\hat{N}_\tau$ the particle-number operator for either neutrons ($\tau = n$) or protons ($\tau = p$), and the angular-momentum projection operator is

$$\hat{P}_{MK}^J = \frac{2J+1}{8\pi^2}\int d\Omega\, D_{MK}^{J*}(\Omega)\hat{R}(\Omega), \tag{22}$$

with $D_{MK}^J(\Omega)$ a Wigner D function. The projector $\hat{P}_{MK}^J$ extracts from the intrinsic state $|\mathbf{q}\rangle$ the component whose angular momentum along the intrinsic z axis is given by K. In the following, we restrict ourselves to axially symmetric deformation, and thus $K = 0$.

We obtain the weight function $f_\alpha^J(\mathbf{q})$ from the variational principle, which leads to the Hill-Wheeler-Griffin equation [46]:

$$\sum_{\mathbf{q}_b}\left[\mathscr{H}_{\mathbf{q}_a,\mathbf{q}_b}^J - E_\alpha^J\mathscr{N}_{\mathbf{q}_a,\mathbf{q}_b}^J\right]f_\alpha^J(\mathbf{q}_b) = 0. \tag{23}$$

The Hamiltonian kernel $\mathscr{H}^J_{\mathbf{q}_a,\mathbf{q}_b}$ and norm kernel $\mathscr{N}^J_{\mathbf{q}_a,\mathbf{q}_b}$ are given by

$$\mathscr{O}^J_{\mathbf{q}_a,\mathbf{q}_b} = \langle NZJ(\mathbf{q}_a)|\hat{O}|NZJ(\mathbf{q}_b)\rangle, \qquad (24)$$

with the operator $\hat{O}$ representing either $\hat{H}$ or 1.

C. Matrix elements for the $0\nu\beta\beta$ decay

Let us now consider the evaluation of the matrix element for the $0\nu\beta\beta$ decay of an initial nuclear state $|\Psi_I(0^+_1)\rangle$ to a final state $|\Psi_F(0^+_1)\rangle$,

$$M^{0\nu} = \langle \Psi_F(0^+_1)|\hat{O}^{0\nu}(0)|\Psi_I(0^+_1)\rangle. \qquad (25)$$

Here, $\hat{O}^{0\nu}(0)$ is the bare, unevolved two-body transition operator [10,12–14] whose form is given by

$$\hat{O}^{0\nu}(0) = \frac{1}{4} \sum_{pp'nn'} O^{pp'}_{nn'} \{A^{pp'}_{nn'}\}, \qquad (26)$$

where p, p' and n, n' are indices for proton and neutron states, respectively.

In the IMSRG+GCM approach, we represent the initial and final states as $|\Psi_{I/F}\rangle = e^{-\hat{\Omega}_{I/F}(s)}|\Phi_{I/F}\rangle$, where the unitary transformations capture correlations that are missing from the GCM wave functions $|\Phi_{I/F}\rangle$. One can readily show that the GCM wave functions are solutions to the Schrödinger equations for the evolved Hamiltonian operators,

$$\hat{H}_{I/F}(s)|\Phi_{I/F}\rangle = E|\Phi_{I/F}\rangle, \qquad (27)$$

up to IMSRG truncation errors (cf. Refs. [24,25]).

The transition matrix element now reads

$$M^{0\nu}(s) = \langle \Phi_F|e^{\hat{\Omega}_F(s)}\hat{O}^{0\nu}(0)e^{-\hat{\Omega}_I(s)}|\Phi_I\rangle, \qquad (28)$$

and we encounter two complications. The first is that $\hat{\Omega}_F(s)$ and $\hat{\Omega}_I(s)$ are normal-ordered with respect to different reference states; this difficulty can be overcome by re-normal-ordering all operators with respect to a common reference. The second, more challenging complication is that the difference between $\hat{\Omega}_I(s)$ and $\hat{\Omega}_F(s)$ prevents us from using a straightforward BCH expansion to evaluate the matrix element. To proceed, we note that we can rewrite Eq. (28) either as

$$M^{0\nu}(s) = \langle \Phi_F|e^{\hat{\Omega}_F(s)}e^{-\hat{\Omega}_I(s)}e^{\hat{\Omega}_I(s)}\hat{O}^{0\nu}(0)e^{-\hat{\Omega}_I(s)}|\Phi_I\rangle$$
$$= \langle \Phi_F|e^{\hat{\Omega}_F(s)}e^{-\hat{\Omega}_I(s)}\hat{O}^{0\nu}_I(s)|\Phi_I\rangle \qquad (29)$$

or

$$M^{0\nu}(s) = \langle \Phi_F|\hat{O}^{0\nu}_F(s)e^{\hat{\Omega}_F(s)}e^{-\hat{\Omega}_I(s)}|\Phi_I\rangle \qquad (30)$$

with $\hat{O}^{0\nu}_{I/F}(s) = e^{\hat{\Omega}_{I/F}}\hat{O}^{0\nu}e^{-\hat{\Omega}_{I/F}}$. Inspecting the unitary transformations acting on the initial GCM wave function in the previous equation, we define

$$|\overline{\Phi}_I\rangle \equiv e^{\hat{\Omega}_F(s)}e^{-\hat{\Omega}_I(s)}|\Phi_I\rangle = e^{\hat{\Omega}_F(s)}|\Psi_I\rangle, \qquad (31)$$

so that we have the unitary transformation for the final nucleus acting on an eigenstate of the initial nucleus. An analogous definition for the final nucleus results from Eq. (29):

$$|\overline{\Phi}_F\rangle \equiv e^{\hat{\Omega}_I(s)}e^{-\hat{\Omega}_F(s)}|\Phi_F\rangle = e^{\hat{\Omega}_I(s)}|\Psi_F\rangle. \qquad (32)$$

Using these newly defined states, we set up two schemes for evaluating the transition matrix element:

PI: $\quad M^{0\nu} = \langle \overline{\Phi}_F|e^{\hat{\Omega}_I}\hat{O}^{0\nu}e^{-\hat{\Omega}_I}|\Phi_I\rangle, \qquad (33)$

PF: $\quad M^{0\nu} = \langle \Phi_F|e^{\hat{\Omega}_F}\hat{O}^{0\nu}e^{-\hat{\Omega}_F}|\overline{\Phi}_I\rangle. \qquad (34)$

More explicitly, the procedures are as follows. We begin with a GCM calculation for the ground state of either the initial nucleus (in procedure PI) or the final nucleus (in procedure PF) to obtain a reference state, and solve the flow equation to obtain the corresponding unitary transformation operator $e^{\hat{\Omega}_I}$ or $e^{\hat{\Omega}_F}$. We then use the unitary transformation to generate the evolved Hamiltonian $\hat{H}_{I/F}(s)$ and decay operator $\hat{O}^{0\nu}_{I/F}(s)$. Finally, we diagonalize the evolved Hamiltonian, approximately, in the other nucleus—the final nucleus in PI and the initial nucleus in PF—to obtain the barred state $|\overline{\Phi}_F\rangle$ or $|\overline{\Phi}_I\rangle$. This second diagonalization—another GCM calculation in our case—would provide an exact result if it and the flow were carried out without approximation. Since the initial and final states are (approximate) eigenvectors of the same Hamiltonian, we can simply sandwich the corresponding evolved $0\nu\beta\beta$ operator between those states, as in Eqs. (33) or (34), to compute $M^{0\nu}$. If we want, we can also use the evolved Hamiltonian to recompute the ground state of the first nucleus, the one for which we solved the flow equations. We will show shortly that both the energies of low-lying states and the matrix elements $M^{0\nu}$ can be improved in this way.

In either of the procedures above, one must use the BCH expansion (17) to transform the charge-changing operator (26). In the present work, we apply the NO2B approximation to each operator appearing in the BCH series, *including* general nested commutators $[\hat{\Omega}, \hat{O}^{0\nu}]^{(n)}$, in the spirit of Ref. [41]. Dropping the flow-parameter dependence for brevity, we see that the first commutator in the series reads

$$[\hat{\Omega}, \hat{O}] = [\hat{\Omega}^{(1)}, \hat{O}] + [\hat{\Omega}^{(2)}, \hat{O}] \qquad (35)$$

$$\equiv \frac{1}{4} \sum_{pp'nn'} \left(O^{pp'}_{nn'}(1\text{B}) + O^{pp'}_{nn'}(2\text{B}) \right) \{A^{pp'}_{nn'}\}, \qquad (36)$$

where the contributions involving the one-body and two-body parts of Ω are given by

$$O^{pp'}_{nn'}(1\text{B}) = \sum_{p_1} \left[\Omega^p_{p_1} O^{p_1 p'}_{nn'} + \Omega^{p'}_{p_1} O^{pp_1}_{nn'} \right]$$
$$- \sum_{n_1} \left[\Omega^{n_1}_n O^{pp'}_{n_1 n'} + \Omega^{n_1}_{n'} O^{pp'}_{nn_1} \right] \qquad (37)$$

and

$$O^{pp'}_{nn'}(2\text{B}) = \frac{1}{2} \sum_{p_1 p_2} \Omega^{pp'}_{p_1 p_2} O^{p_1 p_2}_{nn'} (1 - n_{p_1} - n_{p_2})$$
$$- \frac{1}{2} \sum_{n_1 n_2} O^{pp'}_{n_1 n_2} \Omega^{n_1 n_2}_{nn'} (1 - n_{n_1} - n_{n_2}),$$
$$+ \sum_{p_1 n_1} (n_{p_1} - n_{n_1}) \left[\Omega^{n_1 p'}_{n' p_1} O^{p_1 p}_{n_1 n} - \Omega^{n_1 p}_{n' p_1} O^{p_1 p'}_{n_1 n} \right]$$
$$+ \Omega^{n_1 p}_{np_1} O^{p_1 p'}_{n_1 n'} - \Omega^{n_1 p'}_{np_1} O^{p_1 p}_{n_1 n'}], \qquad (38)$$

(cf. Refs. [24,25]). Since $\hat{\Omega}(s)$ conserves charge, no zero- or one-body terms are generated when we evaluate the commutator (35) (induced higher-body operators are truncated), and the resulting operator has the same isospin structure as the initial transition operator itself. This means that we can use Eqs. (35)–(38) to recursively evaluate the BCH series by replacing $\hat{O}$ with the appropriate nested commutator $[\hat{\Omega}, \hat{O}]^{(n)}$. Correlations in the reference state only enter through fractional values of the occupation numbers, $0 \leqslant n \leqslant 1$. At the currently employed NO2B truncation level, irreducible two- and higher-body density matrices do not appear.

As discussed in Sec. II B, our GCM reference states are projected onto states with good angular momentum, allowing us to efficiently solve our equations by working in a J-coupled scheme. Detailed expressions can be found in Appendix A.

III. RESULTS AND DISCUSSION

A. Energies of low-lying states

Let us now apply the formalism described above to ^{48}Ca and ^{48}Ti, within just the fp shell (comprising the $0f_{7/2}$, $0f_{5/2}$, $1p_{3/2}$, and $1p_{1/2}$ orbits) and with the interaction KB3G [47]. We aim to make our GCM reference states as simple as possible while at the same time including the most important collective correlations. We therefore construct them from a set of axially deformed, angular-momentum- and particle-number-projected HFB states with different values for the quadrupole deformation parameter $\beta_2 \equiv \chi \langle \mathbf{q} | (r/b)^2 Y_{20} | \mathbf{q} \rangle / (\hbar \omega_0)$, with $\hbar \omega_0 = 41.2 A^{-1/3}$ MeV, and $\chi = 0.6$. We let $\beta_2 \in \{-0.3, -0.2, \ldots, 0.2, 0.3\}$ in ^{48}Ca, and $\beta_2 \in \{-0.3, -0.2, \ldots, 0.4, 0.5\}$ in ^{48}Ti. For these axially deformed HFB states, one-dimensional angular-momentum projection, together with particle-number projection, is sufficient to restore all the broken symmetries.

Figure 1 presents curves of HFB energy vs deformation (often referred to as "energy surfaces" even in one dimension) for ^{48}Ca and ^{48}Ti, both before and after projection onto states with $J = 0$ and well-defined particle number. The global energy minimum is at a spherical shape in ^{48}Ca and a prolate shape in ^{48}Ti. The figure also shows the energies of the lowest lying states after the full calculations, which mix the shapes indicated by the dots. The ground states have GCM energies of -7.12 MeV in ^{48}Ca and -22.18 MeV in ^{48}Ti. The results of exact diagonalization are -7.57 and -23.81 MeV, both significantly smaller than the corresponding GCM results. Figure 2 shows that the energies of the low-lying states are fairly stable against different choice of the number of natural states (NOS) in the GCM calculations. In other words, there are good "plateaus" for the energies of both nuclei. The collective wave function for the ground state is, however, somewhat sensitive to the NOS.

Next we solve the IMSRG flow equations, starting both from these GCM states and several simpler states, so that we can check the dependence of the results on the reference. Figure 3 shows the ground-state energy of ^{48}Ca and ^{48}Ti, as a function of the flow parameter, starting from either the spherical projected-HFB state, deformed projected-HFB states with $\beta_2 = 0.1, 0.2, (0.3)$, or the full GCM ground state
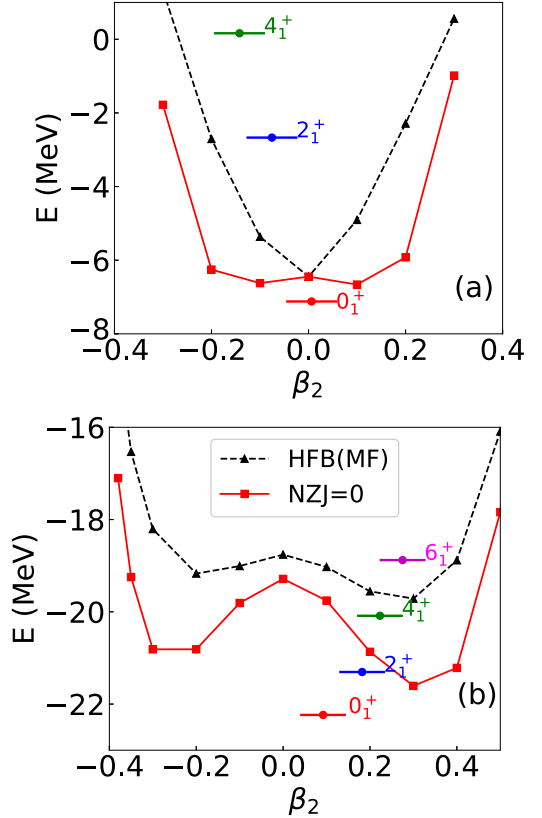

FIG. 1. The energy surface from the projected HFB calculation and the energies of low-lying states in ^{48}Ca (a) and ^{48}Ti (b). The x axis is the quadrupole deformation β_2. Each low-lying state from the GCM calculation is placed at the average β_2 value for that state.

0_1^+. In ^{48}Ca, except when the reference state has $\beta_2 = 0.2$, the energy converges to almost the same value, quite close to the result of exact diagonalization. We note in passing that, as discussed in Refs. [24,25,48] the IMSRG flow may lead to an excited 0^+ state that has a larger overlap with the reference state than the ground state. Because the energy of the reference state with $\beta = 0.2$ is lower than that of the 0_2^+ state, the IMSRG, which cannot raise the energy, does not converge to any sate at all. But we have checked that when we start from a reference state with $\beta_2 = 0.3$, the flow indeed causes the energy to converge to that of the 0_2^+ state.

In ^{48}Ti, only projected-HFB reference states with $\beta \geqslant 0.2$ (and the GCM state) lead to a final energy that is very close to the exact ground-state value. Starting from smaller values of β, we fall short of the correct binding energy. Clearly it is important that the reference state be deformed in the right way; the IMSRG(2) flow by itself is not able to capture collective correlations. The bottom panel also shows that it is important to include three-body irreducible densities in the flow equations. If these are omitted, as the pathological blue open symbols indicate, the energy fails to converge to any value.

The final step in computing low-lying spectra, as we noted earlier, is to use the evolved Hamiltonian from the IMSRG to carry out a second GCM calculation. Figure 4 compares the
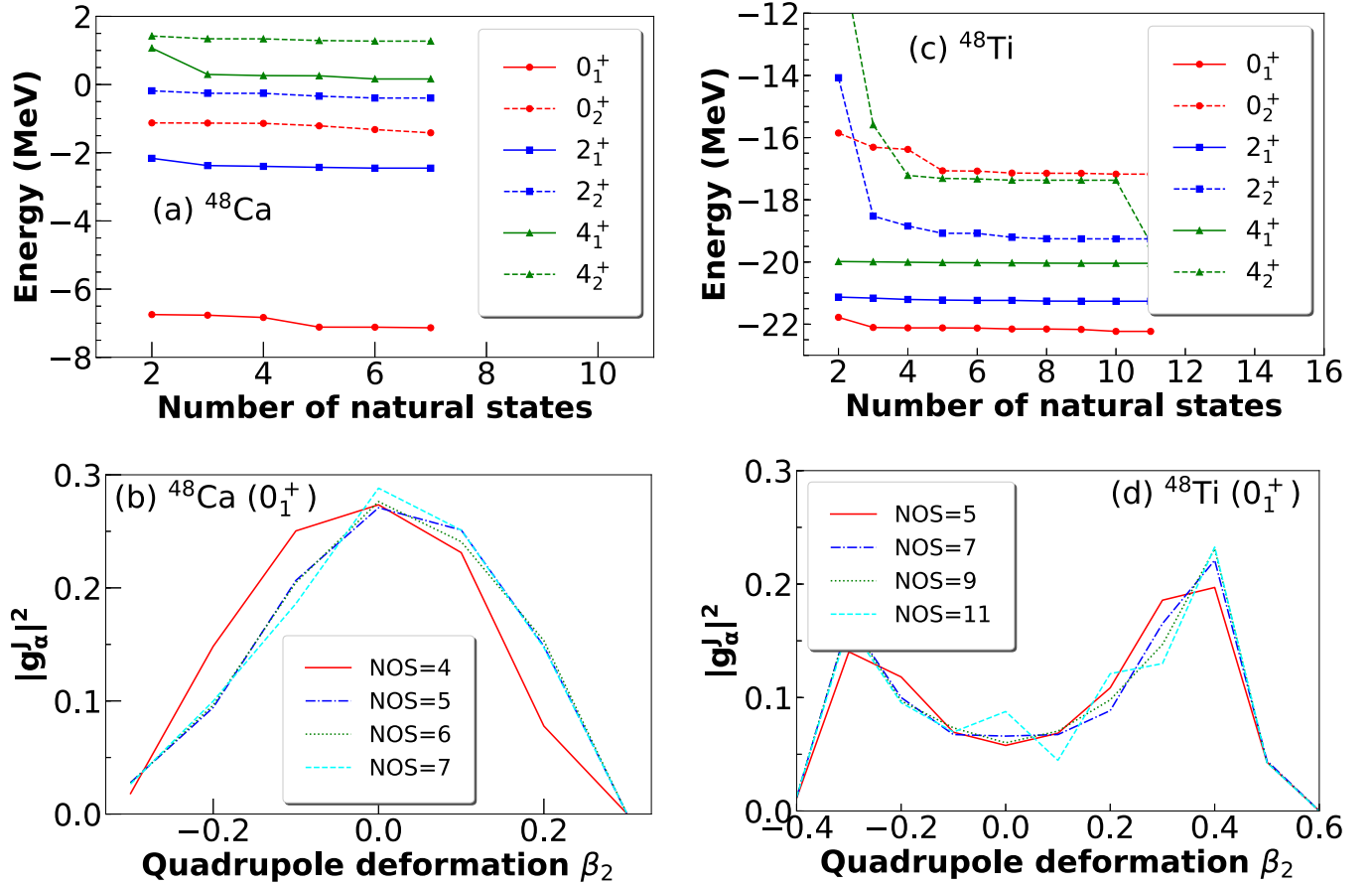
FIG. 2. The energies of low-lying states in ^{48}Ca (a) and ^{48}Ti (c) as a function of the number of natural states (NOS) adopted in the GCM calculations. The collective wave functions, defined as $g_\alpha^J(\beta_2) = \sum_{\beta_2'} [\mathscr{N}^J]_{\beta_2,\beta_2'}^{1/2} f_\alpha^J(\beta_2')$, are shown for different choices of the NOS for the ground state of ^{48}Ca (b) and ^{48}Ti (d), as a function of the quadrupole deformation β_2.

low-lying spectra from an initial GCM calculation, from the second one (labeled IMSRG+GCM), and from exact diagonalization. The IMSRG+GCM energies are systematically lower than those produced by the GCM alone, and are closer to the shell-model results (mostly due to an overall shift). The GCM is capable in principle of reproducing the exact results with a sufficiently high number of coordinates or basis states, but computation time scales badly with the number of coordinates. A more limited GCM calculation, followed by IMSRG evolution and a second limited GCM calculation is much more efficient.

Table I, finally, contains the ground-state energies for ^{48}Ca and ^{48}Ti in several approximation schemes. The IMSRG+GCM overestimates the energy of ^{48}Ti by about 1%. This discrepancy is consistent with other applications of the IMSRG in the NO2B approximation [25], and preliminary results suggest that it can be reduced significantly by using an improved truncation scheme that accounts for induced three-body terms [48].

B. Matrix elements for neutrinoless double beta decay

Figure 5 compares the exact shell model result for the Gamow Teller (GT) part of $M^{0\nu}$ to GCM and IMSRG+GCM

results. The blue boxes represent the results of the PI and PF procedures described above; the vertical extent of the boxes represents the uncertainty in the optimal NOS, i.e., the point at which to truncate the GCM basis before the energy becomes numerically unstable. In the previous GCM studies this uncertainty must also have existed, but was not explicitly investigated. We show here that the matrix elements depend more on the NOS than does the energy. The dependence reflects the similar dependence of the collective wave functions shown in Fig. 2.

The matrix elements produced by the two IMSRG+GCM procedures are in reasonable agreement with one another, and both are slightly closer to the exact result than the value produced by the GCM. The inability of the IMSRG evolution to reduce the matrix element more significantly suggests that it is unable to fully capture isoscalar pairing correlations, which shrink the matrix element noticeably [13,14,50]. The red boxes show the result of including an isoscalar pairing amplitude as a GCM coordinate, in the manner suggested by Refs. [13,14]. Now the agreement with the exact result is good even before the IMSRG evolution, which does not spoil it either. We note that including the isoscalar pairing amplitude as a generator coordinate introduces more redundancy in the basis. By choosing the number of natural states properly, the
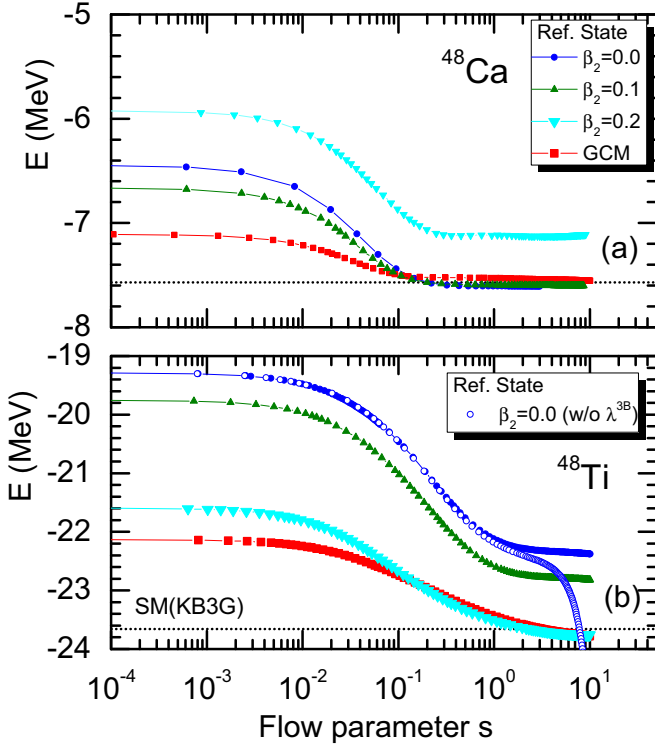
FIG. 3. The ground-state energy E a function of flow parameter s for ^{48}Ca (a) and ^{48}Ti (b), starting from either the spherical reference state, a symmetry-projected HFB state, or a GCM state. The horizontal line represents the energy from exact shell-model diagonalization.

low-lying eigenstates are at energies that are systematically somewhat smaller than without the isoscalar pairing coordinate. Here we have run into the limits of what we can test in a shell-model space. Within the fp shell, collective correlations, which include isoscalar pairing, almost completely determine the $0\nu\beta\beta$ matrix element [50]. Because the IMSRG does not easily capture these correlations, it has little effect on the matrix element; the collective physics must thus all be built into the GCM state, an unsurprising situation. In an *ab initio* calculation in many shells, however, the situation is different. Noncollective correlations from higher energy, including the short-range correlations usually inserted by hand in shell-model calculations, will affect the IMSRG operator evolution. We expect our procedure(s) for computing $0\nu\beta\beta$
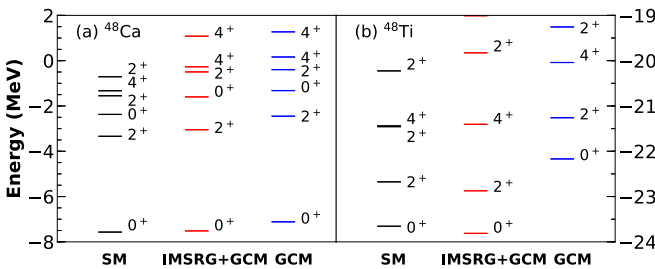

FIG. 4. The low-lying states from the IMSRG+GCM and GCM alone, with the KB3G interaction, in ^{48}Ca (a) and ^{48}Ti (b). The exact shell-model results [49] are on the left in both panels.

TABLE I. Ground-state energies (in MeV) for ^{48}Ca and ^{48}Ti, from several calculations.

	SM	IMSRG+GCM	GCM	HFB(Sph.)
^{48}Ca	−7.57	−7.56	−7.12	−6.45
^{48}Ti	−23.66	−23.81	−22.18	−18.76

matrix elements to work well in these kinds of calculations, even if we are not able to prove it in a single shell.

Although neither IMSRG prescription affects the matrix element very much, PF works slightly less well than PI, a result that is consistent with the IMSRG ground-state energies in the two nuclei. The discrepancy with the exact calculation is larger in ^{48}Ti than in ^{48}Ca, suggesting that the approximate evolution with respect to a complicated GCM state containing both valence neutrons and protons omits some important three-body contributions to the like-particle interaction, which determines the ^{48}Ca energy and wave function.

IV. CONCLUSION

We have presented a very general framework for applying the IMSRG in conjunction with GCM reference states to compute energies of low-lying states and $0\nu\beta\beta$ matrix elements in nuclei with strong collective correlations, including deformation. Our method involves first a GCM calculation to generate a correlated reference state, then an IMSRG calculation, based on that state, to transform all operators, and finally a second GCM calculation that employs those operators. This approach allows us to use a single transformation to treat the transitions between two potentially quite different nuclei.

We have benchmarked our method against the results of exact shell-model diagonalization for ^{48}Ca and ^{48}Ti. The IMSRG improves the GCM-alone energies significantly, and
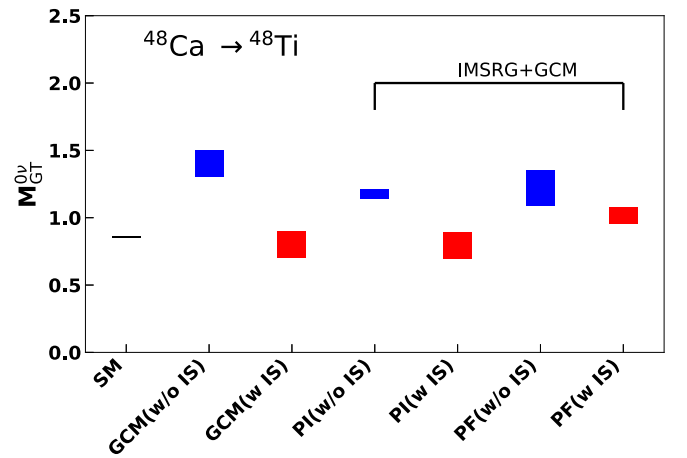

FIG. 5. The Gamow-Teller part of $M^{0\nu}$ from several calculations. The blue boxes (without IS) are results of the GCM and IMSRG+GCM calculations without an explicit isoscalar pairing coordinate, and the red boxes (with IS) are results with that explicit coordinate. The uncertainty comes from the different choice of natural states in the GCM calculation.

the $0\nu\beta\beta$ matrix element slightly, though in the one-shell calculations performed here the GCM correlations by themselves are sufficient (and necessary) to nearly reproduce the exact shell-model matrix element when the coordinates include the isoscalar pairing amplitude. We are in the process of applying the IMSRG+GCM in *ab initio* calculations of this and other decays.

APPENDIX A: *J*-COUPLED OPERATOR EVOLUTION

It is convenient to rewrite the two-body matrix elements in the *J* scheme with the relation [51]

$$|kl\rangle = \sum_{JM} \langle j_k m_k j_l m_l | JM \rangle [N_{KL}(J)]^{-1} |(KL)JM\rangle, \quad \text{(A1)}$$

where the normalized *J*-coupled two-body wave function is defined as

$$|(KL)JM\rangle = N_{KL}(J)[a_K^\dagger a_L^\dagger]_{JM}|0\rangle, \quad \text{(A2)}$$

and the normalization factor is give by $N_{KL}(J) = \sqrt{1 + \delta_{KL}(-1)^J}/(1 + \delta_{KL})$. Here the capital letter K stands for the quantum numbers $\{\tau_k, n_k, l_k, j_k\}$. With the above definition, normalized *J*-coupled nonzero two-body matrix elements are related to those in M scheme as follows:

$$O_{(KL)(34)}^J = \sum_{m_k m_l m_3 m_4} \langle j_k m_k j_l m_l | JM \rangle \langle j_3 m_3 j_4 m_4 | JM \rangle \frac{1}{\sqrt{(1 + \delta_{KL})(1 + \delta_{34})}} O_{34}^{kl}. \quad \text{(A3)}$$

The *unnormalized* versions of the same matrix elements are given by

$$\bar{O}_{(KL)(34)}^J = \sqrt{(1 + \delta_{KL})(1 + \delta_{34})} O_{KL34}^J = \sum_{m_k m_l m_3 m_4} \langle j_k m_k j_l m_l | JM \rangle \langle j_3 m_3 j_4 m_4 | JM \rangle O_{34}^{kl}. \quad \text{(A4)}$$

One can show that the unnormalized *J*-coupled two-body matrix elements corresponding to the first two terms in Eq. (38) (*pp* parts) are given by

$$\bar{\mathcal{O}}_{(KL)(34)}^J(pp) = \frac{1}{2} \sum_{CD} \bar{\Omega}_{(KL)(CD)}^J \bar{O}_{(CD)(34)}^J (1 - n_c - n_d) - \frac{1}{2} \sum_{12} \bar{O}_{(KL)(12)}^J \bar{\Omega}_{(12)(34)}^J (1 - n_1 - n_2), \quad \text{(A5)}$$

and those corresponding to the last two terms in Eq. (38) (*ph* parts) are

$$
\begin{aligned}
\bar{\mathcal{O}}_{(KL)(34)}^J(ph) = {} & -\sum_{J'} \hat{j}'^2 \begin{Bmatrix} j_k & j_l & J \\ j_3 & j_4 & J' \end{Bmatrix} \sum_{A6} (n_6 - n_a) \bar{O}_{(K\bar{4})(6\bar{A})}^{J'} \bar{\Omega}_{(6\bar{A})(3\bar{L})}^{J'} \\
& - (-1)^{j_k + j_l + J + 1} \sum_{J'} \hat{j}'^2 \begin{Bmatrix} j_l & j_k & J \\ j_3 & j_4 & J' \end{Bmatrix} \sum_{A6} (n_6 - n_a) \bar{O}_{(L\bar{4})(6\bar{A})}^{J'} \bar{\Omega}_{(6\bar{A})(3\bar{K})}^{J'} \\
& + \sum_{J'} \hat{j}'^2 \begin{Bmatrix} j_k & j_l & J \\ j_3 & j_4 & J' \end{Bmatrix} \sum_{A6} (n_a - n_6) \bar{\Omega}_{(K\bar{4})(A\bar{6})}^{J'} \bar{O}_{(A\bar{6})(3\bar{L})}^{J'} \\
& + (-1)^{j_k + j_l + J + 1} \sum_{J'} \hat{j}'^2 \begin{Bmatrix} j_l & j_k & J \\ j_3 & j_4 & J' \end{Bmatrix} \sum_{A6} (n_a - n_6) \bar{\Omega}_{(L\bar{4})(A\bar{6})}^{J'} \bar{O}_{(A\bar{6})(3\bar{K})}^{J'}, \quad \text{(A6)}
\end{aligned}
$$

where the Latin indices k, l stand for proton states and the numerals 3,4 stand for neutron states. Only the Ω-matrix elements of the form $\Omega_{n'p'}^{np}$ contribute to the *ph* parts of $\mathcal{O}$. The unnormalized *ph* matrix element $\bar{O}^J$ is related to that of *pp* matrix element $\bar{O}^J$ by the Pandya transformation [51]

$$\bar{O}_{(\alpha\bar{\beta})(\gamma\bar{\delta})}^J = -\sum_{J'} \hat{j}'^2 \begin{Bmatrix} j_\alpha & j_\beta & J \\ j_\gamma & j_\delta & J' \end{Bmatrix} \bar{\mathcal{O}}_{(\alpha\delta)(\gamma\beta)}^{J'}. \quad \text{(A7)}$$

APPENDIX B: THE BRILLOUIN GENERATOR

In the IMSRG(2) calculation, we truncate the matrix elements of $\eta(s)$ at the NO2B level,

$$\hat{\eta}(s) = \sum_{ij} \eta_l^k(s)\{A_l^k\} + \frac{1}{4}\sum_{klmn}\eta_{mn}^{kl}(s)\{A_{mn}^{kl}\}, \tag{B1}$$

and use the Brillouin generator [25]. The matrix elements of the one- and two-body parts are ($\bar{n}_i = 1 - n_i$)

$$\eta_l^k = f_k^l(n_l - n_k) - \frac{1}{2}\sum_{abc}\left(\Gamma_{bc}^{la}\lambda_{bc}^{ka} - \Gamma_{kc}^{ab}\lambda_{lc}^{ab}\right), \tag{B2}$$

$$\eta_{mn}^{kl} = \Gamma_{kl}^{mn}(\bar{n}_k\bar{n}_l n_m n_n - n_k n_l \bar{n}_m \bar{n}_n) + \sum_a \left(f_k^a\lambda_{mn}^{al} + f_l^a\lambda_{mn}^{ka} - f_a^m\lambda_{an}^{kl} - f_a^n\lambda_{ma}^{kl}\right) + \frac{1}{2}\left[(\lambda\Gamma)_{kl}^{mn}(1 - n_k - n_l)\right.$$

$$\left. - (\Gamma\lambda)_{kl}^{mn}(1 - n_m - n_n)\right] + (1 - \hat{P}_{mn})(1 - \hat{P}_{kl})\sum_{ac}\Gamma_{cl}^{am}\lambda_{cn}^{ak}(n_l - n_m) + \frac{1}{2}\sum_{abc}\left[(1 - \hat{P}_{mn})\Gamma_{bc}^{ma}\lambda_{bcn}^{akl} + (1 - \hat{P}_{kl})\Gamma_{lc}^{ab}\lambda_{cmn}^{abk}\right]. \tag{B3}$$

We use the J-coupled scheme above to save memory. Since the terms involving the three-body irreducible density are more complicated than the others, we write them explicitly:

$$\bar{\eta}_{(KL)(MN)}^J(\lambda^{3B}, 1) = \frac{1}{2}\sum_{ABC}\sum_{J_2 J_{ak} J_{bc}}(-1)^{J_{ak} + j_a - j_k}\hat{J}_{ak}\hat{J}_{bc}\hat{J}_2^2(-1)^{J_{ak} + J_{bc} + j_l + j_n}$$

$$\times \begin{Bmatrix} j_a & J_{ak} & j_k \\ j_l & J & J_2 \end{Bmatrix}\begin{Bmatrix} j_a & J_{bc} & j_m \\ j_n & J & J_2 \end{Bmatrix}\bar{\Gamma}_{(MA)(BC)}^{J_{bc}}\langle(j_a j_k)J_{ak}j_l; J_2|\lambda|(j_b j_c)J_{bc}j_n; J_2\rangle, \tag{B4a}$$

$$\bar{\eta}_{KL)(MN)}^J(\lambda^{3B}, 2) = (-1)^{j_m + j_n - J + 1}\frac{1}{2}\sum_{ABC}\sum_{J_{ak} J_{bc}}\sum_{J_2}(-1)^{j_a + J_{ak} - j_k}(-1)^{4j_a + J_{bc} + J_{ak} + 2J + j_m + j_l}\hat{J}_2^2\hat{J}_{bc}\hat{J}_{ak}$$

$$\times \begin{Bmatrix} j_a & J_{ak} & j_k \\ j_l & J & J_2 \end{Bmatrix}\begin{Bmatrix} j_a & J_{bc} & j_n \\ j_m & J & J_2 \end{Bmatrix}\bar{\Gamma}_{(NA)(BC)}^{J_{bc}}\langle(j_a j_k)J_{ak}j_l; J_2|\lambda|(j_b j_c)J_{bc}j_m; J_2\rangle, \tag{B4b}$$

$$\bar{\eta}_{(KL)(MN)}^J(\lambda^{3B}, 3) = \frac{1}{2}\sum_{ABC}\sum_{J_2 J_{ab} J_{cm}}(-1)^{j_c + J_{cm} - j_m}\hat{J}_{ab}\hat{J}_{cm}\hat{J}_2^2(-1)^{J_{ab} + J_{cm} + J + j_l + j_n + 2j_k}$$

$$\times \begin{Bmatrix} j_c & J_{cm} & j_m \\ j_n & J & J_2 \end{Bmatrix}\begin{Bmatrix} j_c & J_{ab} & j_l \\ j_k & J & J_2 \end{Bmatrix}\bar{\Gamma}_{(AB)(LC)}^{J_{ab}}\langle(j_a j_b)J_{ab}j_k; J_2|\lambda|(j_c j_m)J_{cm}j_n; J_2\rangle, \tag{B4c}$$

$$\bar{\eta}_{(KL)(MN)}^J(\lambda^{3B}, 4) = (-1)^{j_k + j_l - J + 1}\frac{1}{2}\sum_{ABC}\sum_{J_{ab} J_{cm} J_2}(-1)^{j_c + J_{cm} - j_m}(-1)^{2j_l + 4j_c + j_k + j_n + J_{ab} + J_{cm} + J}\hat{J}_{cm}\hat{J}_{ab}\hat{J}_2^2$$

$$\times \begin{Bmatrix} j_c & J_{ab} & j_k \\ j_l & J & J_2 \end{Bmatrix}\begin{Bmatrix} j_c & J_{cm} & j_m \\ j_n & J & J_2 \end{Bmatrix}\bar{\Gamma}_{(AB)(KC)}^{J_{ab}}\langle(j_a j_b)J_{ab}j_l; J_2|\lambda|(j_c j_m)J_{cm}j_n; J_2\rangle. \tag{B4d}$$

Here, λ^{3B} in parentheses indicates a dependence on the irreducible three-body density $\langle(j_1 j_2)J_{12}j_3; J|\lambda|(j_4 j_5)J_{45}j_6; J\rangle$, the calculation of which is given in Appendix C.

APPENDIX C: DENSITY MATRICES OF MULTIREFERENCE STATES

We present here the most important expressions needed to compute the density matrices associated with a general multireference state, taken here to have spin and parity 0^+. The irreducible (or residual) one-, two-, and three-body parts of density matrix elements follow from a cumulant expansion (11). In the coupled scheme, the expressions for the one- and two-body densities take the form (with $\kappa = \{n, \alpha\}$)

$$\lambda_{\kappa_1\kappa_2}^{J=0} = \rho_{\kappa_1\kappa_2}^{J=0} \equiv \frac{[a_{\kappa_1}^\dagger \tilde{a}_{\kappa_2}]_0^0}{\sqrt{2j_1 + 1}}\delta_{\alpha_1\alpha_2}. \tag{C1}$$

$$\lambda_{(12)(34)}^J = \rho_{(12)(34)}^J - \lambda_{\kappa_1,\kappa_3}^{J=0}\lambda_{\kappa_2,\kappa_4}^{J=0}\delta_{\alpha_1,\alpha_3}\delta_{\alpha_2,\alpha_4} + (-1)^{J - (j_1 + j_2)}\lambda_{\kappa_1,\kappa_4}^{J=0}\lambda_{\kappa_2,\kappa_3}^{J=0}\delta_{\alpha_1,\alpha_4}\delta_{\alpha_2,\alpha_3}, \tag{C2}$$

where $\alpha = \{\tau l j\}$, and the expression for the irreducible three-body density takes the form

$$\langle (j_1 j_2) J_{12} j_3; J_{123} | \lambda | (j_4 j_5) J_{45} j_6; J_{123} \rangle$$

$$= \sum_{m_1, m_2, \ldots, m_6} \langle j_1 m_1 j_2 m_2 | J_{12} M_{12} \rangle \langle J_{12} M_{12} | j_3 m_3 J M \rangle \langle j_4 m_4 j_5 m_5 | J_{45} M_{45} \rangle \langle J_{45} M_{45} j_6 m_6 | J M \rangle \lambda_{456}^{123}$$

$$= \langle (j_1 j_2) J_{12} j_3; J_{123} | \rho | (j_4 j_5) J_{45} j_6; J_{123} \rangle - \sum_{i=1}^{15} T_i, \tag{C3}$$

where

$$T_1 = (-1)^{J_{45}+j_2+j_3+1} \hat{J}_{12} \hat{J}_{45} \begin{Bmatrix} j_1 & j_2 & J_{12} \\ j_3 & J & J_{45} \end{Bmatrix} \rho_{\kappa_1 \kappa_6}^{J=0} \rho_{(23)(45)}^{J_{45}}, \tag{C4a}$$

$$T_2 = \sum_{J_{23}} (-1)^{J_{45}+J_{23}+j_1+j_2+j_3+j_4} \hat{J}_{12} \hat{J}_{45} \hat{J}_{23}^2 \begin{Bmatrix} j_4 & j_1 & J_{45} \\ J & j_6 & J_{23} \end{Bmatrix} \begin{Bmatrix} j_2 & j_3 & J_{23} \\ J & j_1 & J_{12} \end{Bmatrix} \rho_{\kappa_1 \kappa_5}^{J=0} \rho_{(23)(64)}^{J_{23}}, \tag{C4b}$$

$$T_3 = \sum_{J_{23}} (-1)^{j_2+j_3+j_5+j_6} \hat{J}_{12} \hat{J}_{45} \hat{J}_{23}^2 \begin{Bmatrix} j_5 & j_1 & J_{45} \\ J & j_6 & J_{23} \end{Bmatrix} \begin{Bmatrix} j_2 & j_3 & J_{23} \\ J & j_1 & J_{12} \end{Bmatrix} \rho_{\kappa_1 \kappa_4}^{J=0} \rho_{(23)(56)}^{J_{23}}, \tag{C4c}$$

$$T_4 = (-1)^{j_1+j_2-J_{12}+1} \hat{J}_{12} \hat{J}_{45} \begin{Bmatrix} j_2 & j_1 & J_{12} \\ j_3 & J & J_{45} \end{Bmatrix} \rho_{\kappa_2 \kappa_6}^{J=0} \rho_{(31)(45)}^{J_{45}}, \tag{C4d}$$

$$T_5 = \sum_{J_{31}} (-1)^{j_4+j_1+J_{12}+J_{45}+1} \hat{J}_{12} \hat{J}_{45} \hat{J}_{31}^2 \begin{Bmatrix} j_4 & j_2 & J_{45} \\ J & j_6 & J_{31} \end{Bmatrix} \begin{Bmatrix} j_1 & j_3 & J_{31} \\ J & j_2 & J_{12} \end{Bmatrix} \rho_{\kappa_1 \kappa_4}^{J=0} \rho_{(31)(64)}^{J_{31}}, \tag{C4e}$$

$$T_6 = \sum_{J_{31}} (-1)^{j_1+j_2+J_{12}+j_5+j_6+J_{31}} \hat{J}_{12} \hat{J}_{45} \hat{J}_{31}^2 \begin{Bmatrix} j_5 & j_2 & J_{45} \\ J & j_6 & J_{31} \end{Bmatrix} \begin{Bmatrix} j_1 & j_3 & J_{31} \\ J & j_2 & J_{12} \end{Bmatrix} \rho_{\kappa_2 \kappa_4}^{J=0} \rho_{(31)(56)}^{J_{31}}, \tag{C4f}$$

$$T_7 = \delta_{J_{12} J_{45}} \rho_{\kappa_3 \kappa_6}^{J=0} \rho_{(12)(45)}^{J_{12}}, \tag{C4g}$$

$$T_8 = (-1)^{j_3+j_4+J_{45}+1} \hat{J}_{12} \hat{J}_{45} \begin{Bmatrix} j_4 & j_3 & J_{45} \\ J & j_6 & J_{12} \end{Bmatrix} \rho_{\kappa_3 \kappa_5}^{J=0} \rho_{(12)(64)}^{J_{12}}, \tag{C4h}$$

$$T_9 = (-1)^{J_{12}+j_5+j_6+1} \hat{J}_{12} \hat{J}_{45} \begin{Bmatrix} j_5 & j_3 & J_{45} \\ J & j_6 & J_{12} \end{Bmatrix} \rho_{\kappa_3 \kappa_4}^{J=0} \rho_{(12)(56)}^{J_{12}}, \tag{C4i}$$

$$T_{10} = -2 \hat{J}_{12} \hat{J}_{45} \begin{Bmatrix} j_1 & j_2 & J_{12} \\ j_3 & J & J_{45} \end{Bmatrix} \rho_{\kappa_1 \kappa_6}^{J=0} \rho_{\kappa_2 \kappa_5}^{J=0} \rho_{\kappa_3 \kappa_4}^{J=0}, \tag{C4j}$$

$$T_{11} = -2(-1)^{J_{45}+j_2+j_3+1} \hat{J}_{12} \hat{J}_{45} \begin{Bmatrix} j_1 & j_2 & J_{12} \\ j_3 & J & J_{45} \end{Bmatrix} \rho_{\kappa_1 \kappa_6}^{J=0} \rho_{\kappa_2 \kappa_4}^{J=0} \rho_{\kappa_3 \kappa_5}^{J=0}, \tag{C4k}$$

$$T_{12} = -2(-1)^{j_1+j_2-J_{12}+1} \hat{J}_{12} \hat{J}_{45} \begin{Bmatrix} j_2 & j_1 & J_{12} \\ j_3 & J & J_{45} \end{Bmatrix} \rho_{\kappa_1 \kappa_5}^{J=0} \rho_{\kappa_2 \kappa_6}^{J=0} \rho_{\kappa_3 \kappa_4}^{J=0}, \tag{C4l}$$

$$T_{13} = 2(-1)^{j_1+j_2-J_{12}} \delta_{J_{12} J_{45}} \rho_{\kappa_1 \kappa_5}^{J=0} \rho_{\kappa_2 \kappa_4}^{J=0} \rho_{\kappa_3 \kappa_6}^{J=0}, \tag{C4m}$$

$$T_{14} = 2(-1)^{j_2+j_3-J_{12}+J_{45}} \hat{J}_{12} \hat{J}_{45} \begin{Bmatrix} j_2 & j_1 & J_{12} \\ j_3 & J & J_{45} \end{Bmatrix} \rho_{\kappa_1 \kappa_4}^{J=0} \rho_{\kappa_2 \kappa_6}^{J=0} \rho_{\kappa_3 \kappa_5}^{J=0}, \tag{C4n}$$

$$T_{15} = -2 \delta_{J_{12} J_{45}} \rho_{\kappa_1 \kappa_4}^{J=0} \rho_{\kappa_2 \kappa_5}^{J=0} \rho_{\kappa_3 \kappa_6}^{J=0}. \tag{C4o}$$

[1] F. T. Avignone III, S. R. Elliott, and J. Engel, Rev. Mod. Phys. **80**, 481 (2008).

[2] P. Vogel, J. Phys. G: Nucl. Part. Phys. **39**, 124002 (2012).

[3] Y. Iwata, N. Shimizu, T. Otsuka, Y. Utsuno, J. Menendez, M. Honma, and T. Abe, Phys. Rev. Lett. **116**, 112502 (2016).

[4] R. A. Sen'kov and M. Horoi, Phys. Rev. C **93**, 044334 (2016).

[5] J. Menendez, A. Poves, E. Caurier, and F. Nowacki, Nucl. Phys. A **818**, 139 (2009).

[6] J. Barea, J. Kotila, and F. Iachello, Phys. Rev. C **91**, 034304 (2015).

[7] M. T. Mustonen and J. Engel, Phys. Rev. C **87**, 064302 (2013).

[8] F. Šimkovic, V. Rodin, A. Faessler, and P. Vogel, Phys. Rev. C **87**, 045501 (2013).

[9] J. Hyvarinen and J. Suhonen, Phys. Rev. C **91**, 024613 (2015).

[10] T. R. Rodríguez and G. Martinez-Pinedo, Phys. Rev. Lett. **105**, 252503 (2010).

[11] N. L. Vaquero, T. R. Rodriguez, and J. L. Egido, Phys. Rev. Lett. **111**, 142501 (2013).

[12] L. S. Song, J. M. Yao, P. Ring, and J. Meng, Phys. Rev. C **90**, 054309 (2014); J. M. Yao, L. S. Song, K. Hagino, P. Ring, and J. Meng, *ibid.* **91**, 024316 (2015); L. S. Song, J. M. Yao, P. Ring, and J. Meng, *ibid.* **95**, 024305 (2017).

[13] N. Hinohara and J. Engel, Phys. Rev. C **90**, 031301 (2014).

[14] C. F. Jiao, J. Engel, and J. D. Holt, Phys. Rev. C **96**, 054310 (2017).

[15] D. L. Fang, A. Faessler, and F. Šimkovic, Phys. Rev. C **97**, 045503 (2018).

[16] J. Engel and J. Menendez, Rep. Prog. Phys. **80**, 046301 (2017).

[17] D. Lee, Prog. Part. Nucl. Phys. **63**, 117 (2009).

[18] P. Navratil, S. Quaglioni, I. Stetcu and B. R. Barrett, J. Phys. G **36**, 083101 (2009).

[19] V. Somà, C. Barbieri, and T. Duguet, Phys. Rev. C **89**, 024323 (2014).

[20] B. R. Barrett, P. Navratil, and J. P. Vary, Prog. Part. Nucl. Phys. **69**, 131 (2013).

[21] G. Hagen, T. Papenbrock, M. Hjorth-Jensen, and D. J. Dean, Rep. Prog. Phys. **77**, 096302 (2014).

[22] J. Carlson, S. Gandolfi, F. Pederiva, S. C. Pieper, R. Schiavilla, K. E. Schmidt, and R. B. Wiringa, Rev. Mod. Phys. **87**, 1067 (2015).

[23] K. D. Launey, T. Dytrych, and J. P. Draayer, Prog. Part. Nucl. Phys. **89**, 101 (2016).

[24] H. Hergert, S. K. Bogner, T. D. Morris, A. Schwenk, and K. Tsukiyama, Phys. Rep. **621**, 165 (2016).

[25] H. Hergert, Phys. Scr. **92**, 023002 (2017).

[26] K. Tsukiyama, S. K. Bogner, and A. Schwenk, Phys. Rev. Lett. **106**, 222502 (2011).

[27] K. Tsukiyama, S. K. Bogner, and A. Schwenk, Phys. Rev. C **85**, 061304 (2012).

[28] S. K. Bogner, H. Hergert, J. D. Holt, A. Schwenk, S. Binder, A. Calci, J. Langhammer, and R. Roth, Phys. Rev. Lett. **113**, 142501 (2014).

[29] S. R. Stroberg, H. Hergert, J. D. Holt, S. K. Bogner, and A. Schwenk, Phys. Rev. C **93**, 051301 (2016).

[30] S. R. Stroberg, A. Calci, H. Hergert, J. D. Holt, S. K. Bogner, R. Roth, and A. Schwenk, Phys. Rev. Lett. **118**, 032502 (2017).

[31] T. D. Morris, J. Simonis, S. R. Stroberg, C. Stumpf, G. Hagen, J. D. Holt, G. R. Jansen, T. Papenbrock, R. Roth, and A. Schwenk, Phys. Rev. Lett. **120**, 152503 (2018).

[32] N. M. Parzuchowski, S. R. Stroberg, P. Navratil, H. Hergert, and S. K. Bogner, Phys. Rev. C **96**, 034324 (2017).

[33] W. Kutzelnigg and D. Mukherjee, J. Chem. Phys. **107**, 432 (1997).

[34] D. Mukherjee, Chem. Phys. Lett. **274**, 561 (1997).

[35] L. Kong, M. Nooijen, and D. Mukherjee, J. Chem. Phys. **132**, 234107 (2010).

[36] H. Hergert, S. Binder, A. Calci, J. Langhammer, and R. Roth, Phys. Rev. Lett. **110**, 242501 (2013).

[37] H. Hergert, S. K. Bogner, T. D. Morris, S. Binder, A. Calci, J. Langhammer, and R. Roth, Phys. Rev. C **90**, 041302(R) (2014)

[38] E. Gebrerufael, K. Vobig, H. Hergert, and R. Roth, Phys. Rev. Lett. **118**, 152503 (2017).

[39] W. Magnus, Commun. Pure Appl. Math. **7**, 649 (1954).

[40] S. Blanes, F. Casas, J. Oteo, and J. Ros, Phys. Rep. **470**, 151 (2009).

[41] T. D. Morris, N. M. Parzuchowski, and S. K. Bogner, Phys. Rev. C **92**, 034331 (2015).

[42] G. Hagen, D. J. Dean, M. Hjorth-Jensen, T. Papenbrock, and A. Schwenk, Phys. Rev. C **76**, 044305 (2007).

[43] R. Roth, S. Binder, K. Vobig, A. Calci, J. Langhammer, and P. Navratil, Phys. Rev. Lett. **109**, 052501 (2012).

[44] E. Gebrerufael, A. Calci, and R. Roth, Phys. Rev. C **93**, 031301 (2016).

[45] G. Hagen, G. R. Jansen, and T. Papenbrock, Phys. Rev. Lett. **117**, 172501 (2016).

[46] P. Ring and P. Schuck, *The Nuclear Many-Body Problem* (Springer, Berlin, 1980).

[47] A. Poves, J. Sanchez-Solano, E. Caurier, and F. Nowacki, Nucl. Phys. A **694**, 157 (2001).

[48] H. Hergert, J. M. Yao, T. D. Morris, N. M. Parzuchowski, S. K. Bogner, and J. Engel, J. Phys.: Conf. Ser. **1041**, 012007 (2018).

[49] P. Van Isacker, J. Engel, and K. Nomura, Phys. Rev. C **96**, 064305 (2017).

[50] J. Menendez, N. Hinohara, J. Engel, G. Martinez-Pinedo, and T. R. Rodriguez, Phys. Rev. C **93**, 014305 (2016).

[51] J. Suhonen, *From Nucleons to Nucleus. Concepts of Microscopic Nuclear Theory*, 1st ed. (Springer, Berlin, 2007).